Smith, M. J. T. and House, M. E., "Internally Generated Noise From Gas Turbine Engines, Measurement and Prediction," *Transactions of ASME: Journal of Engineering for Power*, 1967.

Smith, E. B. et al., "Study and Tests to Reduce Compressor Sounds of Jet Aircraft," TR DS-68-7, contract FA65WA-1236 to FAA, 1968, General Electric Co., Cincinnati, Ohio.

Schaut, L. A., "Results of an Experimental Investigation of Total Pressure Performance and Noise Reduction of an Airfoil Grid Inlet," document D6-23276, 1969, Boeing Co., Seattle, Wash.

Putnam, T. W. and Smith, R. H., "XB-70 Compressor-Noise Reduction and Propulsion-System Performance for Choked Inlet Flow," TND-5692, 1970, NASA.

Anderson, R., DeStafanis, P., Farquhar, B. W., Giarda, G., Shuehle, A., and VanDuine, A. A., "Boeing/Aeritalia Sonic Inlet Feasibility Study," document D6-40208, 1972, Boeing Co., Seattle, Wash.

Chestnutt, D., "Noise Reduction by Means of Inlet-Guide-Vane Choking in an Axial-Flow-Compressor," TND-4682, 1968, NASA.

Lumsdaine, E., "Development of a Sonic Inlet for Jet Aircraft," *Internoise '72 Proceedings*, Inst. of Noise Control Engineering, Washington, D.C., 1972, pp. 501–506.

OCTOBER 1973 J. AIRCRAFT VOL. 10, NO. 10

Static Aeroelasticity and the Flying Wing

Terrance A. Weisshaar*
University of Maryland
College Park, Md.
and
Holt Ashley†
National Science Foundation
Washington, D.C.

This paper demonstrates, by means of elementary examples, certain features of flying wing static aeroelasticity. Prominent among these are the influence of trimming control surfaces on wing divergence. Models are formulated using elementary beam-rod differential equations and aerodynamic strip theory. Divergence of an unswept wing, rolling freely about a pinned shaft, is discussed. The resulting torsional divergence speed is nearly three times that of a nonrolling wing of half the span, clamped at the root. If the rolling velocity of the full wing is trimmed by elevons, antisymmetrical divergence may occur at a speed lower than the classical torsional divergence speed. The case of a wing trimmed in roll by 30% Fowler flaps is presented. A similar elementary analysis of an oblique or yawed wing free to roll about a pinned shaft parallel to an airstream and trimmed in roll is also presented. Considering only wing bending flexibility, it is found, through the application of Galerkin's method, that the application of ailerons to trim roll results in a divergence q five times that of a similar symmetrical sweptforward wing clamped at the center. Finally, a similar freely flying yawed wing is trimmed in pitch and roll by elevons such that the total lift equals the aircraft weight. It is found that the divergence q which occurs in this case is nearly twelve times that of the clamped symmetrical sweptforward wing.

Introduction

VEHICLES based on the flying wing arrangement, or something closely approximating it, have engaged in manned, powered flight for at least as far back as 1910. Gibbs-Smith[1] describes the Dunne No. 5 Tailless of that date, and his historical review also encompasses the Hill Pterodactyl of 1926, the Lippisch Tailless Research Monoplane of 1931 and others. More familiar is the series of scaled and experimental aircraft which culminated in the Northrop XB-35 (Fig. 1) and XB-49; details on them can be found, for instance, in Janes' for 1948.[2] At about the same time, in Great Britain, Armstrong Whitworth Aircraft Limited were testing the A.W. 52 series.[3]

Although the objects of great enthusiasm by their protagonists, none of the early flying wings seems to have evolved into a successful operational aircraft. There are several reasons for their failures, but two appear most prominent. The first was the extreme difficulty of achieving satisfactory unaugmented handling qualities, control and dynamic stability, especially in the lateral-directional modes. An excellent summary of the state of knowledge about this problem during World War II is given by Donlan.[4] The second is that they simply were not big enough. As observed also by Donlan[4] flying wings of that era allowed inadequate provision for payload and only "for large airplanes having spans of 150–500 ft, the volume of the wing alone may be sufficient to enclose bulk or weight of an appreciable magnitude even with the thin wing sections required for high speed."

It is worth mentioning that the 1940's generation of tailless vehicles attained what might be described as moderate subsonic performance. Thus Janes[2] cites a speed of 350 mph for the rocket-powered Northrop MX-324, whereas Murray[3] estimates a maximum of 500 mph at sea level (including compressibility effects) for the A. W. 52 (E9/44) with two Nene 1 turbojets. The corresponding range of dynamic pressures, coupled with the fact that their struc-

Presented as Paper 73-397 at the AIAA/ASME/SAE 14th Structures, Structural Dynamics, and Materials Conference, Williamsburg, Va., March 20–22, 1973; submitted April 3, 1973; revision received July 26, 1973. The authors are indebted to G. C. C. Smith, Bell Aerospace Corporation, Buffalo, N.Y., for alerting them to the relationship between their analyses and those in Refs. 13–16. This research was supported in part by the Air Force Office of Scientific Research, Contract F44620-68-C-0036 and the NASA-ASEE Summer Faculty Fellowship Program at Ames Research Center, Calif., June 19–August 25, 1972.

Index categories: Aircraft Handling, Stability, and Control; Aeroelasticity and Hydroelasticity; Aircraft Structural Design (Including Loads).

*Assistant Professor, Aerospace Engineering Department, Virginia Polytechnic Institute and State University, Blacksburg, Va. Associate Member AIAA.

†Director, Office of Exploratory Research and Problem Assessment, (on leave of absence from School of Engineering, Stanford University). Fellow AIAA.

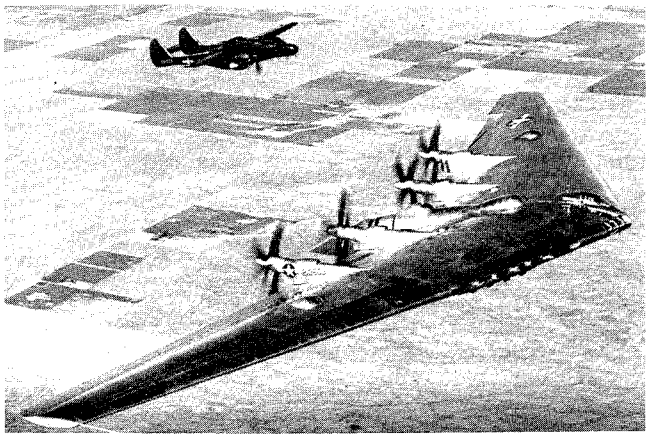

Fig. 1 Northrop XB-35 flying wing.

tures were quite conservatively designed, probably accounts for the absence of any difficulty with aeroelastic phenomena on these aircraft. A rich archival literature, full of interesting discussions on performance, stability and control, contains no reference that the authors have been able to find, even to something as critical as flutter.

The flying wing is now experiencing a revival, and there is excellent cause to raise the question of what aeroelastic problems may be encountered on the 1970's generation of designs. The present paper propounds a few tentative answers, drawn from studies of highly simplified cases that lend themselves to elementary mathematical treatment. There is obviously no attempt to arrive at quantitative results applicable to any real configuration, since the principal aim is to examine whether the flying wing may behave differently from what one might expect based on experience with more conventional situations.

Because its spanwise distributions of lift and inertia are nearly in proportion, a tailless aircraft with its payload and fuel properly spread across the span imposes only very mild internal loads on its structure during gust encounters, maximum pull-ups, pushovers and the like. If, additionally, use is made of air cushion support or a multiplicity of landing gears, as in at least two current studies (Refs. 5, 6; Fig. 2) then loads due to landing and ground operation will similarly be minimized. It follows that an unusually high proportion of the structural components will be sized by considerations of stiffness and aeroelasticity.

Among other factors favoring the reappearance of these vehicles are improved automatic control and stabilization technology, which promises reliably to ensure the required handling qualities; the trend to very large size, which leads to acceptable payload volumes through the square-cube law; and the attractiveness of lowered structural weight fraction. Takeoff gross weights of one to two million pounds are being seriously envisioned, and the unfavorable influence of increasing size on this last parameter[7] will drive the designer to the better internal-loads situation mentioned above. Again the aeroelastician's job is likely to be exacerbated.

Perhaps the most curious contemporary development relative to the flying wing involves a family of arrangements based on the asymmetric oblique wing concept of Jones.[8,9] These include both designs with relatively conventional fuselage and tail (Fig. 3) and tailless. Figure 4 shows a wind-tunnel model which, according to Jones,[9] is representative of a flying wing with transonic and low supersonic lift-to-drag ratios well above 10. Such values are achieved, in combination with excellent low-speed performance, by taking off in the unswept configuration but cruising at sweep angles between 50° and 60°.

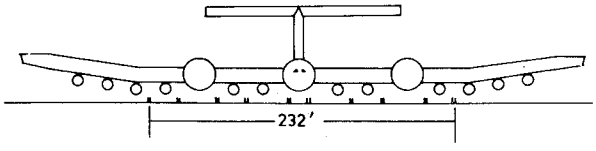

Fig. 2 Frontal view of proposed Boeing resources transport showing landing gear arrangement (Ref. 5).

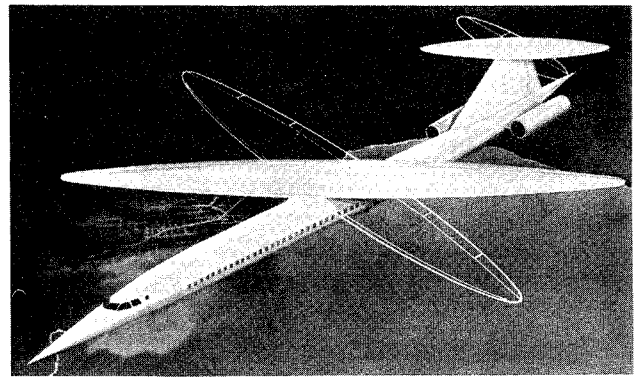

Fig. 3 Artist's concept of proposed NASA oblique wing transport aircraft.

No reference is made here to questions of stability and trim. It is a matter of keen concern, however, to ask what the familiar combination of high dynamic pressure and transonic Mach number may mean to aeroelastic behavior. One question that immediately comes to mind is whether the swept arrangement, without fuselage or separate trimming surface, will benefit from the favorable influence of sweepback on bending-torsion divergence or suffer the deterioration in divergence speed that is the bugaboo of sweptforward wings with bilateral symmetry.

Static vs Dynamic Aeroelasticity

Based on a first round of elementary studies, it is the authors' belief that no unpleasant surprises are likely to

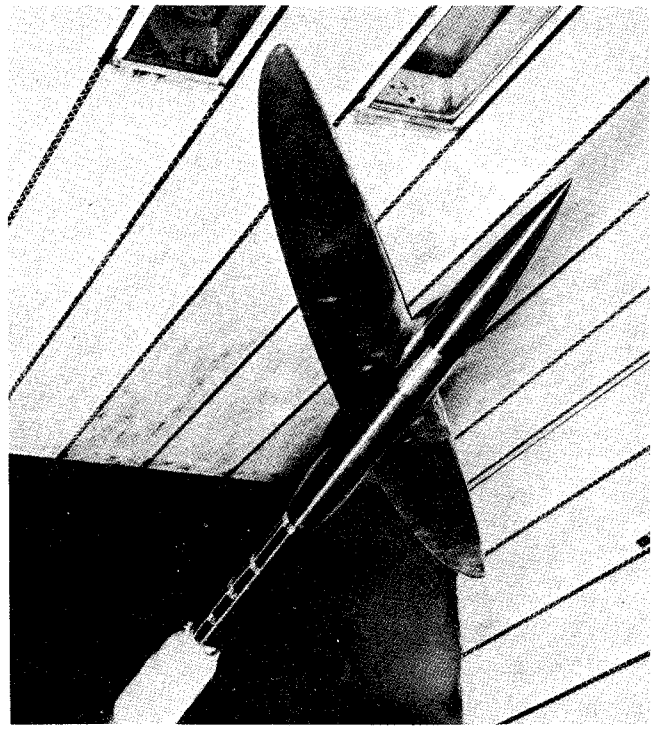

Fig. 4 Oblique wing model in NASA Ames Research Center 11 ft. wind tunnel.

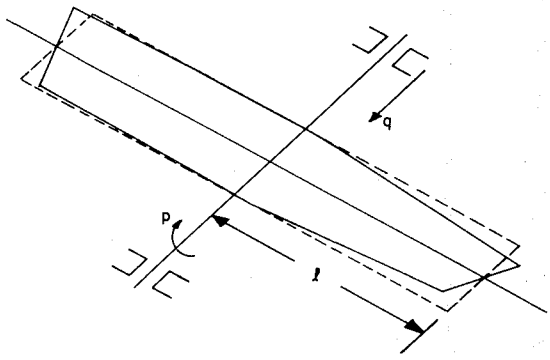

Fig. 5 Uniform unswept wing, deformed antisymmetrically, rolling about an axis parallel to the flight direction.

be encountered in connection with dynamic aeroelastic phenomena like flutter and gust response. This is not to say that high-performance designs do not have to be subjected to the customary sequence of analyses, wind tunnel tests and flight tests that precedes flutter clearance of any other vehicle. It is quite likely, in fact, that more structural material will have to be added to a static-loads designed flying wing,‡ in order to attain acceptable flutter margins, than might be needed on a conventional aircraft with similar flight envelope, gross weight, limit load factor, aspect ratio, etc. The point is that nothing really new is expected.

This conclusion can be explained by looking at the frequency spectrum of comparable flying and conventional wings. If primary flexure-torsion flutter is under study, one recalls that the single most significant controlling parameter for wings is the fundamental natural frequency of torsional vibration, with the first bending frequency an important second. Let the two wings be idealized, respectively, as a uniform, free-free beam-rod of span $2l$ and an equally stiff and massive cantilever beam-rod of span l, the latter representing either half of the conventional wing encastré in a heavy fuselage. Then, in the absence of appreciable coupling between bending and torsion, one easily determines from the properties of such rods[10] that, not only are the lowest torsional frequencies equal in both cases, but so are all pairs of higher harmonics.

For bending vibration, the free-free fundamental turns out to have a frequency 39.5% greater than that of the cantilever. Unless the former is so high that an accidental near-coincidence with torsion tends to depress the flutter speed, one can reason that primary flutter performance will be roughly the same in the two cases.

There are, however, several qualifications. For instance, fundamental torsion of the free-free beam-rod involves an antisymmetrical mode with a single node at the center, whereas fundamental bending is symmetrical. If the vehicle has true bilateral symmetry, therefore, one must go to higher modes and examine all potentially critical symmetrical and antisymmetrical flutter couplings. The net effect of these observations is believed to be favorable for flying wing flutter relative to the conventional aircraft. On the other hand, the foregoing assumption of equal running inertias and stiffnesses on the two comparable wings is questionable, because of the milder internal-loads environment on the flying wing. After preliminary design, it is certain to possess a much less rigid structure than its conventional counterpart.

‡Provided that the undesirable practice is followed of sizing the structure for static loads first. In these, as in many other designs, it is much more rational to treat aeroelastic effects in parallel rather than in series with other conditions.

Three Elementary Solutions

Early in the studies leading to this paper, it became clear that the role of trimming control surfaces on static stability or divergence is a uniquely important feature of tailless aeroelasticity. It is perhaps of some interest to describe, with quantitative examples, the line of reasoning which underlies this discovery.

To begin with, it is well known[11] that a uniform, unswept cantilever wing has the divergence dynamic pressure

$$q_D = \left(\frac{\pi}{2l}\right)^2 \left(\frac{GJ}{cea_0}\right) \tag{1}$$

As with all cases treated in this paper, aerodynamic strip theory is assumed. Other properties are as follows:

l = semispan from root to tip.
GJ = torsional rigidity
c = chordlength
e = distance by which the straight elastic axis lies behind the line of aerodynamic centers (assumed straight along a constant percentage chordline)
a_0 = lift-curve slope

With suitable factors to adjust for three-dimensional aerodynamic effects and for spanwise variations of these properties, Eq. (1) characterizes well the parametric dependencies of cantilever torsional divergence. It is, of course, only an implicit formula when one must account for the variations of a_0 and e with Mach number.

On a flying wing, Eq. (1) is inapplicable. There is no fuselage to restrain twist to zero at the root, and the pilot, attempting to trim moments about the c.g., would apply elevon control in response to twisting. In order to construct eigenvalues equivalent to Eq. (1), one finds it necessary to separate symmetrical and antisymmetrical motions. In some ways the latter is more revealing. For this reason, it is treated first.

Imagine a uniform tailless configuration flying at such a low angle of attack that some control input or gust encounter could produce a significant twist θ which is an odd (antisymmetrical) function of spanwise coordinate y. This behavior resembles that of a wind tunnel model (Fig. 5) mounted at its centerline on a streamwise pin, whose bearings restrain pitch and yaw but permit freedom in roll.

In the absence of elevon applications, the twist $\theta(y)$ gives rise to a rolling velocity p. If p is taken positive so as to depress the right wing, a resultant (small) antisymmetrical angle-of-attack distribution occurs.

$$\Delta\alpha(y) = \theta(y) + py/V \tag{2}$$

Let it be assumed that rolling velocities and accelerations are sufficiently small that centrifugal and other inertial effects are negligible. One can then hypothesize that the wing reaches an equilibrium where the rolling moments due to $\theta(y)$ and p add to zero. In terms of previous symbols, the differential equation governing the antisymmetrical part of the twist will be

$$GJ(d^2\theta/dy^2) + (qcea_0)[\theta + py/V] = 0 \tag{3}$$

For future convenience, Eq. (3) is immediately made dimensionless in terms of the independent variable

$$n \equiv y/l \tag{4}$$

With

$$k^2 \equiv \frac{qcel^2a_0}{GJ} \tag{5}$$

and the prime denoting η-differentiation, it reads

$$\theta'' + k^2\left[\theta + \frac{pl}{V}\eta\right] = 0 \tag{6}$$

Boundary conditions on $\theta(\eta)$ suitable for the circumstances in Fig. 5 are

$$\theta(0) = 0 = \theta'(\pm 1) \tag{7}$$

The requirement that p be constant

$$\text{ROLLING MOMENT} \sim \int_0^1 \left[\theta(\eta) + \frac{pl}{V}\eta\right]\eta d\eta = 0 \tag{8}$$

allows p to be eliminated from Eq. (6). The resulting linear integro-differential equation is, from Eq. (6)

$$\theta'' + k^2\left[\theta - 3\eta\int_0^1 \theta(\eta_1)\eta_1 d\eta_1\right] = 0 \tag{9}$$

where η_1 is a dummy spanwise integration variable.

Together, Eqs. (7) and (9) amount to an eigenvalue problem for antisymmetrical divergence with free rolling. Almost by inspection, a solution which gives zero centerline twist is

$$\theta = A\eta + B\sin k\eta \tag{10}$$

the tip condition Eq. (7) yields a relation

$$A = -Bk\cos k \tag{11}$$

between the constants. Finally, when Eqs. (10) and (11) are substituted into Eq. (9), the characteristic equation

$$\tan k = k \tag{12}$$

is found to be the requirement on the system parameters to permit nonzero θ. Table 1 lists the positive solutions of Eq. (12), put in correspondence with the integers.

Only the fundamental eigenvalue has physical interest. It shows a divergence dynamic pressure 8.18 times the cantilever value from Eq. (1). In the absence of compressibility effects on e and a_0, this means the antisymmetrical instability would appear at a speed higher by the factor of 2.86 than where symmetrical divergence might be observed on the Fig. 5 model.

The next question is whether the phenomenon just analyzed has any relationship to actual divergence on a freely flying tailless airplane. That it probably does not can be seen by adding elevon control to the picture. For simplicity, suppose that the uniform wing has full-span trailing-edge elevons (Fig. 6), so segmented and actuated that a constant control rotation angle δ_0, unaffected by elastic twisting, can be maintained relative to the local cross section at all stations across either half span. Let $\delta(\eta)$ represent this elevon angle, and recall that, under strip theory, it produces changes both in lift at the aerodynamic center and in twisting moment about that center. The corresponding aerodynamic derivatives are here abbreviated $c(L_\delta)$ and $c(M_\delta)$. Under these hypotheses, and with $p = 0$, Eq. (6) should be replaced by

$$\theta'' + k^2\theta + \left(\frac{k^2}{a_0}\right)\left[c(L_\delta) + \frac{c}{e}c(M_\delta)\right]\delta = 0 \tag{13}$$

where only the torques due to twist and the elevon are included.

Table 1 Rolling Divergence Eigenvalues

Order	k_{CRIT}
1	$4.493 = 2.86\,(\pi/2)$
2	7.725
3	10.904
4	14.066
5	17.221
6	20.371
7	23.519
$N > 7$	$(2N + 1)\,(\pi/2)$ to within 0.1%

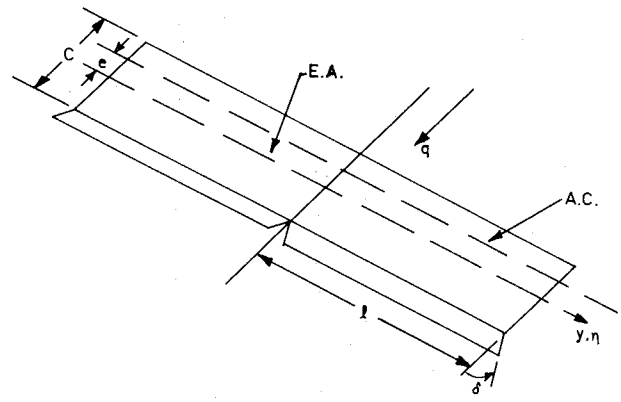

Fig. 6 Uniform wing with full span elevons.

Again the antisymmetrical case is considered first. To counteract an antisymmetrical twist, the pilot or wing-leveler autopilot would apply just enough elevon

$$\delta(\eta) = \delta_0\{\text{sign }\eta\} \tag{14}$$

to ensure zero rolling moment. With $\theta(-\eta) = -\theta(\eta)$, the corresponding dimensionless condition

$$\text{ROLLING MOMENT} \sim \int_0^1 [a_0\theta + c(L_\delta)\delta]\eta d\eta = 0 \tag{15}$$

yields

$$\delta(\eta) = -\frac{2a_0}{c(L_\delta)}\{\text{sign }\eta\}\int_0^1 \theta\eta d\eta \tag{16}$$

the differential equation becomes

$$\theta'' + k^2\left\{\theta - f[\text{sign }\eta]\int_0^1 \theta(\eta_1)\eta_1 d\eta_1\right\} = 0 \tag{17}$$

where

$$f \equiv 2\left[\frac{c}{e}(c(M_\delta)/c(L_\delta)) + 1\right] \tag{18}$$

Boundary conditions Eq. (7) are applicable.

Equation (17) calls for a solution both odd in η and capable of accounting for the discontinuity in running torque at the centerline. To obtain $\theta(0) = 0$, one is led to try

$$\theta = A\sin k\eta + B[\text{sign }\eta][1 - \cos k\eta] \tag{19}$$

The first two derivatives of Eq. (19) are

$$\theta'(\eta) = Ak\cos k\eta + 2B\Delta(\eta)[1 - \cos k\eta] + Bk\,\text{sign}\eta[\sin k\eta] \tag{20}$$

$$\theta''(\eta) = -Ak^2\sin k\eta + Bk^2[\text{sign }\eta][\cos k\eta] + 4Bk\Delta(\eta)\sin k\eta + 2B\Delta'(\eta)[1 - \cos k\eta] \tag{21}$$

Here $\Delta(\eta)$ is the Dirac delta function of unit area. Since Eqs. (20) and (21) reveal no physically unrealizable behavior of the internal torque, one employs the tip boundary condition from Eq. (7) to obtain

$$A = -B\tan k \tag{22}$$

Substitution of Eqs. (19, 21 and 22) into Eq. (17) then produces a characteristic equation for k. One convenient form reads

$$f = \frac{2k\cos k}{[2 + k^2]\cos k - 2} \tag{23}$$

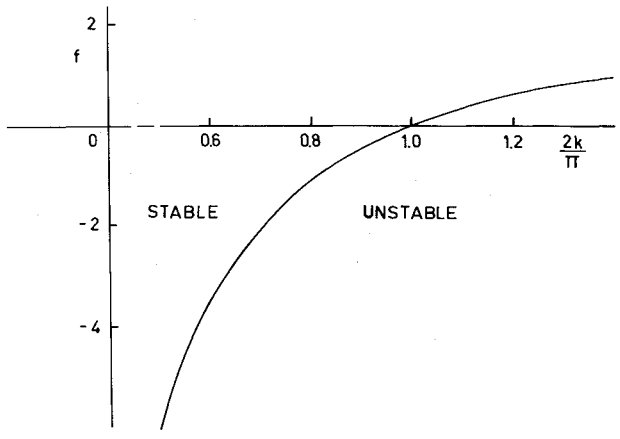

Fig. 7 Fundamental divergence parameter $2k/\pi$ vs wing parameter f.

The roots of Eq. (23) refer to antisymmetrical "torsion-elevon divergence" with trim in roll. Their dependence on the various parameters is extremely interesting. To begin with, there is an intermediate condition $f = 0$, for which the lowest $k_{CRIT} = \pi/2$ corresponds to the cantilever divergence of Eq. (1). More generally, Fig. 7 shows how the fundamental eigenvalue varies with f, which may be positive or negative on actual wings. There are clearly circumstances—for example when the aerodynamic center and elastic axis are close together so that e is small—where the unfavorable wing twist due to the elevons may generate instability at very low speeds indeed. One curious fact about Fig. 7 is that $f = 0$ is a crossover value where the dynamic pressures for cantilever divergence and control reversal are just equal. $f < 0$ goes with the more common (subsonic) case of $q_R < q_D$, and conversely.

Figure 8 presents the specific example of a Fowler-type of control surface with chord equal to 30% of c. Subsonic aerodynamic data were taken from Appendix B.2 of Etkin.[12] The divergence eigenvalue is here plotted vs the ratio e/c; with the aerodynamic center along the quarter-chordline, the variations may be thought of as due to changes in the structural box, which cause the elastic axis to be displaced chordwise.

It is natural to wonder whether there is a symmetrical counterpart to the divergence just studied. An analogous calculation calls for assuming $\theta(-\eta) = \theta(\eta)$, then adjusting δ_0 and the centerline angle of attack α_0 so that, 1) Pitching moment about a spanwise axis through the vehicle c.g. vanishes, and 2) The trimmed lift coefficient is

$$C(L_0) = W/qS \tag{24}$$

where W is total weight and S the reference wing area. If the effect of α_0 is added, the differential equation governing elastic twist becomes

$$\theta'' + k^2[\theta + \alpha_0] + \frac{k^2}{a_0}\left[c(L_\delta) + \frac{c}{e}c(M_\delta)\right]\delta = 0 \tag{25}$$

Again the conditions Eq. (7) apply, the first really amounting to a reference definition for α_0.

It is a simple matter to derive the following equations for lift and moment equilibrium, respectively.

$$\alpha_0 + \frac{c(L_\delta)}{a_0}\delta_0 = \frac{W}{2qSa_0} - \int_0^1 \theta d\eta \tag{26}$$

$$\alpha_0 + \frac{C(M_\delta)}{C(M_\alpha)}\delta_0 = -\int_0^1 \theta d\eta \tag{27}$$

(Here the sectional aerodynamic derivatives with capital C refer to the c.g. axis rather than the aerodynamic center.) When Eq. (27) is subtracted from Eq. (26), one finds

$$\delta_0 = \frac{W}{2qS}\left(\frac{C(M_\alpha)}{c(L_\delta)C(M_\alpha) - a_0C(M_\delta)}\right) \tag{28}$$

that is, the elevon angle for trim is apparently unaffected by wing twisting.

The angle of attack from Eqs. (26), (27) is

$$\alpha_0 = -\frac{W}{2qS}\left(\frac{C(M_\delta)}{c(L_\delta)C(M_\alpha) - a_0C(M_\delta)}\right) - \int_0^1 \theta d\eta \tag{29}$$

Inserting Eqs. (28) and (29) into Eq. (25), one derives the nonhomogeneous equation

$$\theta'' + k^2\left[\theta - \int_0^1 \theta(\eta_1)d\eta_1\right] = K \tag{30}$$

where

$$K = k^2C(L_0)\left[\frac{C(M_\alpha)}{c(L_\delta)C(M_\alpha) - a_0C(M_\delta)}\right]\left[1 - \frac{c}{e}\frac{c(M_\delta)}{a_0} - \frac{c(L_\delta)}{a_0}\right] \tag{31}$$

Thorough examination of the eigenvalue problem implicit in Eq. (7) and (30) has led to the characteristic relation

$$k \sin k = 0 \tag{32}$$

Thus divergence is first found to occur at

$$k_{CRIT} = \pi \tag{33}$$

which is exactly twice the value found (Eq. 1) for the cantilever. This rather disappointing result is quite independent of nearly all the aerodynamic details of the unswept flying wing. It demonstrates that trim requirements affect only the antisymmetric instabilities of this configuration and that the latter are likely to be more significant for structural integrity.

This symmetrical case deserves further study. For one thing, it is worth noting that, if three-dimensional aerodynamics are included, the two integrals will not necessarily cancel when Eq. (27) is subtracted from Eq. (26). δ_0 will depend on the twist distribution, and one will then be led to the physically more reasonable conclusion that the pilot or automatic control system can influence symmetrical divergence.

Before leaving this section it is worth noting that static aeroelastic studies on trimmed conventional and low-aspect ratio configurations have been conducted previously by Hancock.[13-16] These studies bear a close resemblance to those just presented for high-aspect ratio configurations. In general, the eigenvalues characterized herein as

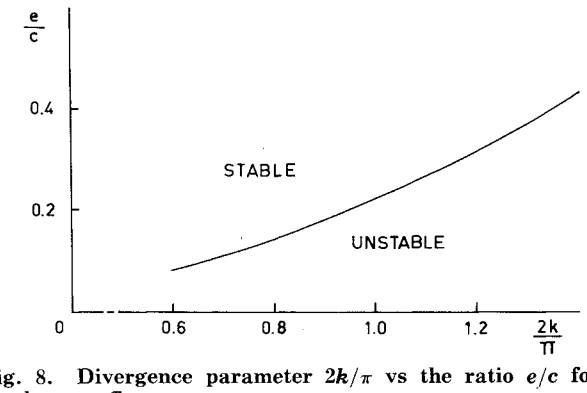

Fig. 8. Divergence parameter $2k/\pi$ vs the ratio e/c for a Fowler-type flap.

divergences correspond to the stability boundaries for Hancock's small displacements from aeroelastic equilibrium. These displacements are analyzed, of course, under prescribed constraints such as a requirement that rolling or pitching moments be continually balanced.

Oblique Wing Response to Elevon Input

The case of a flying wing with its flight direction at an angle to the centerline of the craft presents an interesting question as to whether its behavior will be dominated by the strong tendency to bending-torsion divergence of its sweptforward half or by the extreme static stability of the sweptback half. The behavior of an oblique wing differs from that of the unswept wing in that bending deformations of the oblique wing induce aerodynamic loads in addition to those normally caused by wing torsional deformation. The result is that bending and torsional deformation are coupled. A discussion of swept wing aeroelasticity can be found in Chap. 8 of Ref. 10.

To simplify the aeroelastic analysis of the oblique wing, it will be assumed that the wing is rigid in torsion, in which case only bending flexibility is important. Figure 9 shows the configuration to be examined. If chordwise cross-sections are used and elevons of the type previously described for the unswept wing are included, the governing differential equation for bending is found to be[10]

$$\frac{d^4w}{d\eta^4} + \lambda \frac{dw}{d\eta} \tan\Lambda - \beta\delta(\eta) = 0 \qquad (34)$$

$$-1 \leq \eta \leq 1$$

where

λ = qc $a_0 l^3 \cos^2\Lambda/EI$
β = qc $c_{l\delta} l^3 \cos^2\Lambda/EI$
$w(\eta)$ = bending deformation of elastic axis, non-dimensionalized with respect to l, positive upward
$\delta(\eta)$ = elevon deflection angle, positive downward

A disturbance which causes upward elastic deflection of both halves of the wing will induce a rolling moment about an axis parallel to the airstream and a pitching moment about a perpendicular axis. This effect occurs because the deflection $w(\eta)$ of the sweptforward half generates additional lift on a wing cross-section proportional to $-w'(\eta)\tan\Lambda$, while upward deflection on the sweptback half causes a decrease in lift proportional to $w'(\eta)\tan\Lambda$. If the wing were clamped at its center, the sweptforward half would encounter bending divergence at a dynamic pressure[10] equal to

$$q(D_0) = \frac{6.33EI}{cl^3 a_0 \sin\Lambda \cos\Lambda} \qquad (35)$$

The clamped sweptback wing cannot diverge unless torsional deformation is permitted.

It should be noted that Eq. (34) represents the governing equation for equilibrium in terms of $w(\eta)$ and that $w(\eta)$ represents a perturbation deflection away from a previously trimmed equilibrium configuration. Several events might cause this perturbation deformation and, in turn, cause the aeroelastic rolling moment. One such event is the in-flight sweeping of the wing from one angle to another. As the wing is swept, the sweptforward half acquires a positive increment of aeroelastic lift, while the sweptback portion generates a negative increment of aeroelastic lift. To counteract this aeroelastically induced roll, a trim condition involving ailerons is required.

On the sweptforward half, further elastic deformation caused by the aileron reinforces that aileron, allowing that aileron to furnish powerful control. Conversely, on the sweptback portion, further elastic deformation reduces the aileron effectiveness and, if bending and torsional flexibility are present, a reversal condition may be encountered. The amount of aileron input is, of course, a function of the geometry and elasticity of the wing.

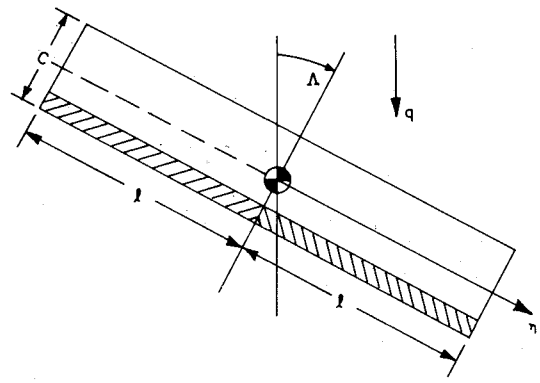

Fig. 9 Oblique flying wing with full span elevons, yawed at an angle Λ to the airstream.

Control of An Oblique Wing Free to Roll About a Pin

Consider first an oblique wing, of the type shown in Fig. 9, mounted on a pinned shaft, parallel to the airstream and passing through the wing c.g., which restrains motion in pitch and yaw, but which permits rolling motion. The requirement that the aeroelastically induced rolling moment be balanced by aileron/elevon displacement is

$$\int_{-1}^{1} \delta(\eta)\eta d\eta + \frac{a_0}{c(l_\delta)} \int_{-1}^{1} \alpha_e(\eta)\eta d\eta = 0 \qquad (36)$$

where $\alpha_e(\eta) = -dw/d\eta \tan\Lambda$
If it is assumed that

$$\delta(\eta) = \begin{cases} \delta_0 & 0 < \eta \leq 1 \\ -\delta_0 & -1 \leq \eta < 0 \end{cases} \qquad (37)$$

then, from Eq. (36)

$$\delta_0 = \frac{a_0}{c(l_\delta)} \tan\Lambda \int_{-1}^{1} \frac{dw}{d\eta}\eta d\eta \qquad (38)$$

Equation (34) may be divided and written in two regions, one valid for the sweptforward half ($-1 \leq \eta < 0$) and the other valid for the sweptback half ($0 < \eta \leq 1$). Equations (37) and (38) may be substituted for $\delta(\eta)$ in each equation. These differential equations become integro-differential equations.

$$\frac{d^4w}{d\eta^4} + \lambda \tan\Lambda\left(\frac{dw}{d\eta} - \int_{-1}^{1} \frac{dw}{d\eta}\eta d\eta\right) = 0 \qquad (39)$$

for

$$0 < \eta \leq 1$$

and

$$\frac{d^4w}{d\eta^4} + \lambda \tan\Lambda\left(\frac{dw}{d\eta} + \int_{-1}^{1} \frac{dw}{d\eta}\eta d\eta\right) = 0 \qquad (40)$$

for

$$-1 \leq \eta < 0$$

The boundary conditions for the problem are that no shear force or bending moment exist at the wing tips

$$\frac{d^3w}{d\eta^3} = 0 = \frac{d^2w}{d\eta^2} \text{ at } \eta = \pm 1 \qquad (41)$$

In addition, since the problem is now written as two coupled equations, the solution for $w(\eta)$ must be geometrically continuous at $\eta = 0$. A general solution to this problem, somewhat like that found for the bending divergence of

the clamped sweptforward wing, is known to exist. However, the characteristic equation which results from satisfaction of boundary conditions makes the exact solution to the problem very involved and time consuming. Thus, that effort is deferred to the future.

An approximate solution can be obtained with relative ease through application of the Galerkin procedure to Eqs. (39) and (40). The deflected shape of a cantilever, uniformly loaded and free from shear and bending moment at the tip, is found to be

$$\psi_R = \frac{1}{3}(6\eta^2 - 4\eta^3 + \eta^4) \tag{42}$$

for a cantilever located in the region $\eta > 0$, and

$$\psi_L = \frac{1}{3}(6\eta^2 + 4\eta^3 + \eta^4) \tag{43}$$

for a cantilever located in the region $\eta < 0$. As assumed deflected shapes for the Galerkin method, let $w_R(\eta)$, the deflection for $\eta > 0$, be

$$w_R(\eta) = A\psi_R(\eta) \tag{44}$$

and, for $w_L(\eta)$, the deflection for $\eta < 0$,

$$w_L(\eta) = B\psi_L(\eta) \tag{45}$$

A and B are undetermined constants. Both w_R and w_L satisfy the tip boundary conditions and lead to geometric continuity at $\eta = 0$. The bending moment and shear which are obtained from w_L and w_R are discontinuous at $\eta = 0$ unless $A = B$. It is worthwhile to note that the application of $w_L(\eta)$ to the Galerkin solution to the bending divergence problem for a uniform sweptforward wing, clamped at the root, yields a value for $q(D_0)$ which is 1.1% higher than the value given in Eq. (35).

When $\psi_R(\eta)$ and $\psi_L(\eta)$ are used as weighting functions for their respective equations, the result of the Galerkin procedure is two simultaneous algebraic equations.

$$\begin{bmatrix} 1 + \frac{13}{160}\lambda\tan\Lambda & -\frac{3}{40}\lambda\tan\Lambda \\ \frac{3}{40}\lambda\tan\Lambda & 1 - \frac{13}{160}\lambda\tan\Lambda \end{bmatrix} \begin{Bmatrix} A \\ B \end{Bmatrix} = \begin{Bmatrix} 0 \\ 0 \end{Bmatrix} \tag{46}$$

The requirement that A and B be nonzero results in a characteristic equation in λ. The solution to this characteristic equation is

$$\lambda_D = \pm 32/\tan\Lambda \tag{47}$$

The plus/minus sign simply says that the value λ_D occurs for $\pm\ \Lambda$ since the wing is elastically symmetric along the η axis. From the definition of λ, the critical dynamic pressure for static divergence of the oblique wing due to this aileron input is

$$q_D = \frac{32EI}{cl^3 a_0 \sin\Lambda\cos\Lambda} \tag{48}$$

or, from Eq. (35)

$$q_D = 5.06q(D_0) \tag{49}$$

Although the result in Eq. (49) appears favorable as compared to the value $q(D_0)$, Diederich and Budiansky show in Ref. 17 that, in some cases and considering both bending and torsion flexibility, at an angle equal to 45° the divergence $q(D_0)$ is only about 5% of its unswept value. Thus, one might conclude, at the very least, that the use of trimming surfaces on an oblique wing is a problem of some importance. The reader is cautioned, however, that the result in Eq. (49) is somewhat qualitative in nature, since it is the result of an approximate solution to a simplified problem. A more definitive solution should include bending and torsion flexibility and three-dimensional aerodynamics. It is interesting to note that the eigenvector for this case gives $B = 1.5A$. The bending divergence mode is a deflection pattern in which both wing halves deflect upward as expected, but the sweptforward half experiences deformations 50% larger than its counterpart.

Elevon Control of a Freely Flying Oblique Wing

If the oblique wing shown in Fig. 9 is free to roll, pitch and translate, elevon input is necessary to trim the wing properly. The situation is similar to that discussed previously for the unswept wing. Taking α_0 as the positive nose-up rigid body rotation about a pitch axis along the η − axis and allowing only bending flexibility, the condition for trimmed lift is

$$\int_{-1}^{1}(\alpha_0 - w'\tan\Lambda)d\eta + \frac{c(l_\delta)}{a_0}\int_{-1}^{1}\delta(\eta)d\eta = \frac{2W}{qSa_0\cos^2\Lambda} \tag{50}$$

This relation is similar to Eq. (26). If, once more, one denotes sectional aerodynamic derivatives with respect to the c.g. axis with capital C, the equation for pitching moment equilibrium becomes

$$\int_{-1}^{1}(\alpha_0 - w'\tan\Lambda)d\eta + \frac{C(M_\delta)}{C(M_\alpha)}\int_{-1}^{1}\delta(\eta)d\eta = 0 \tag{51}$$

This equation is similar to Eq. (27). Moment equilibrium about the centerline axis, yawed at an angle Λ to the airstream, is found to be satisfied if

$$\int_{-1}^{1}(\alpha_0 - w'\tan\Lambda)\eta d\eta + \frac{c(l_\delta)}{a_0}\int_{-1}^{1}\delta(\eta)\eta d\eta = 0 \tag{52}$$

If the assumption is made that

$$\delta(\eta) = \begin{cases} \delta_R & 0 < \eta \le 1 \\ \delta_L & -1 \le \eta < 0 \end{cases}$$

where δ_R and δ_L are constants, then from Eqs. (50–52)

$$\alpha_0 = \left[\frac{W}{qS\cos^2\Lambda}\right]\left[\frac{C(M_\delta)}{a_0 C(M_\delta) + c(l_\delta)C(M_\alpha)}\right] + \frac{\tan\Lambda}{2}\int_{-1}^{1}w'd\eta \tag{53}$$

$$\delta_R = \left[\frac{W}{qS\cos^2\Lambda}\right]\left[\frac{C(M_\alpha)}{c(l_\delta)C(M_\alpha) - a_0 C(M_\delta)}\right] + \left\{\frac{a_0}{c(l_\delta)}\tan\Lambda\right\}\int_{-1}^{1}w'\eta d\eta \tag{54}$$

$$\delta_L = \left[\frac{W}{qS\cos^2\Lambda}\right]\left[\frac{C(M_\alpha)}{c(l_\delta)C(M_\alpha) - a_0 C(M_\alpha)}\right] - \left\{\frac{a_0}{c(l_\delta)}\tan\Lambda\right\}\int_{-1}^{1}w'\eta d\eta \tag{55}$$

As in the example discussed previously in this section, Eq. (34) may be written in two separate regions. The governing equations for the sweptback and sweptforward sec-

tions become, respectively

$$\frac{d^4w}{d\eta^4} + \lambda \tan\Lambda \left(\frac{dw}{d\eta} - 1/2 \int_{-1}^{1} \frac{dw}{d\eta} d\eta + \int_{-1}^{1} \frac{dw}{d\eta} \eta d\eta \right) = \frac{WI^2}{2EI[a_0 C(M_\delta) - c(l_\delta) C(M_\alpha)]} \quad (56)$$

$$\frac{d^4w}{d\eta^4} + \lambda \tan\Lambda \left(\frac{dw}{d\eta} - 1/2 \int_{-1}^{1} \frac{dw}{d\eta} d\eta - \int_{-1}^{1} \frac{dw}{d\eta} \eta d\eta \right) = \frac{WI^2}{2EI[a_0 C(M_\delta) - c(l_\delta) C(M_\alpha)]} \quad (57)$$

The boundary conditions Eq. (41) of zero shear and bending moment at the wing tips and geometric continuity at $\eta = 0$ again apply here. The eigenvalue problem implicit in the homogeneous solution to Eqs. (56) and (57) undoubtedly has an analytic solution. It may be worthwhile to note that $w(\eta)$ = constant is a homogeneous solution to Eqs. (56) and (57). This corresponds to a rotation about the centerline.

If the search for an analytical solution is postponed and, instead, an approximate Galerkin solution is applied, once more using the deflected shape functions Eqs. (44) and (45), the algebraic equations which result are

$$\begin{bmatrix} 1 + \frac{3}{160} \lambda \tan\Lambda & -\frac{1}{80} \lambda \tan\Lambda \\ \frac{1}{80} \lambda \tan\Lambda & 1 - \frac{3}{160} \lambda \tan\Lambda \end{bmatrix} \begin{Bmatrix} A \\ B \end{Bmatrix} = \begin{Bmatrix} 0 \\ 0 \end{Bmatrix} \quad (58)$$

Since A and B must be nonzero, a second order characteristic equation in λ is found.

The roots are

$$\lambda_{cr} = \frac{\pm 32(5)^{1/2}}{\tan\Lambda} \quad (59)$$

Once again, the $\pm$ sign occurs because of elastic symmetry. A comparison of q_D, in this case, with $q(D_0)$ reveals that

$$q_D = 11.3\, q(D_0) \quad (60)$$

The mode shape for instability is found to be

$$\begin{Bmatrix} A \\ B \end{Bmatrix} = \begin{Bmatrix} 1 \\ 2.62 \end{Bmatrix} \quad (61)$$

Thus, the sweptforward wing is deflected upward over two and one-half times as much as its sweptback counterpart.

A comparison of the result given in Eq. (60) with the result in Eq. (49) shows that q_D for the freely flying wing that elevons is about twice that of the constrained wing with elevon roll trimming. It seems that the stability of the sweptback half contributes greatly to the stability of the over-all wing. Once again, however, the reader is reminded of the physical and mathematical approximations used in this study. A much more sophisticated, detailed analysis is necessary on an actual vehicle.

Conclusions

The results presented here involve idealizations such that they are no more than indicative of the expected static aeroelastic behavior of flying wings. Actual vehicle configurations display both spanwise variations of all their properties and finite-span aerodynamic effects. Equally important is the tendency of real control-surface actuators to saturate§ under the large hinge moments experienced at high dynamic pressures. Thus, what are referred to as instabilities in this paper, influenced by control trimming, in actuality lead, not to structural failures, but to large amounts of twist and bending or loss of control effectiveness.

The novelty of the present results may be challenged on the grounds that any thorough numerical analysis of tailless aeroelasticity, which properly introduces all requirements of vehicle equilibrium, will automatically reveal deformations and instabilities like those studied here. It is only in the simple light of understanding that they may contain that the foregoing solutions have potential value.

With these *caveats*, the following conclusions may be listed for the idealized models studied:

1) A wing of span $2l$ with constant roll velocity p, rolling about a pinned shaft parallel to the flight direction, has a torsional divergence speed 2.86 times that of a similar wing of semi-span l clamped at the root and restrained in roll.

2) The use of full-span elevons to trim an unswept wing, in roll only, can lead to an antisymmetrical condition. Divergence can occur above or below the classical torsional divergence speed depending on the wing geometric and aerodynamic parameters.

3) The use of elevons to trim lift and pitch of an unswept wing results in a symmetric divergence condition, but at a speed twice that of the classical torsional divergence speed.

4) Elevon/aileron trimming in roll of an oblique wing results in a bending instability at a dynamic pressure about five times the value of the bending divergence q for a similar sweptforward wing of half the span, clamped at the root, but without elevon/aileron control. Although the conventional divergence of the sweptforward wing would occur first [Eq. (35)], this elevon interaction result is nonetheless important from the standpoint of aircraft controllability. Without the use of aileron or elevon control, the oblique winged aircraft will have a tendency to roll due to aeroelastically induced forces. To date, this phenomenon has not been observed in any wind tunnel model tests.[18] This is obviously due to the fact that the governing stiffness parameter EI/cl^3 is so large as to make the tunnel model aeroelastically rigid with respect to this phenomenon. Further studies detailing the magnitude and severity of these control inputs are presently under study by one of the authors.

5) Elevon trim of an oblique wing for lift, roll and pitch causes bending divergence at a q over 11 times that of the sweptforward half, clamped at the root. This larger value found for full elevon control is consistent with that found for the similar unswept case above.

However, a more detailed analysis, including additional degrees of freedom, more sophisticated aerodynamics and realistic structural modeling is necessary before rigorous conclusions can be drawn. It is hoped that these results will provide the base and the impetus for such studies.

References

[1]Gibbs-Smith, C. H., *Aviation, An Historical Survey from its Origins to the End of World War II,* Her Majesty's Stationery Office, London, 1970.

[2]*Janes All the World's Aircraft,* McGraw-Hill, New York, 1948, pp. 305c–397c.

[3]Murray, C. V., "Full Scale Research on a Flying Wing," *Aircraft Engineering,* Vol. XXI, No. 243, May 1949, pp. 144–148, 158.

§One of the authors recently encountered a design for which both ailerons and horizontal-stabilizer differential are used for rolling. At high speeds, actuator saturation is relied upon to prevent reversed ailerons from overpowering the stabilizer. The reader can judge for himself the desirability of this practice.

[4]"An Interim Report on the Stability and Control of Tailless Airplanes," Rept. 796, 1944, NACA.
[5]"Canada Weighs Arctic Resources Airlift," *Aviation Week and Space Technology*, Vol. 96, No. 21, May 22 1972, pp. 25–26
[6]Unpublished data on a Lockheed Aircraft Corporation "Span Loader" supplied by Dr. Brent Silver.
[7]Cleveland, F. A., "Size Effects in Conventional Aircraft Design," *Journal of Aircraft*, Vol. 7, No. 6, Nov.–Dec. 1970, pp. 483–512.
[8]Jones, R. T., "Reduction of Wave Drag by Antisymmetric Arrangements of Wings and Bodies," *AIAA Journal*, Vol. 10, No. 2, Feb. 1972, pp. 171–176.
[9]Jones, R. T., "New Design Goals and a New Shape for the SST," *Astronautics and Aeronautics*, Vol. 10, No. 12, Dec. 1972, pp. 66–70.
[10]Bisplinghoff, R. L., Ashley, H., and Halfman, R. L., *Aeroelasticity*, Addison-Wesley, Reading, Mass., 1955.
[11]Bisplinghoff, R. L. and Ashley, H., *Principles of Aeroelasticity*, John Wiley and Sons, New York, 1962.
[12]Etkin, B., *Dynamics of Flight; Stability and Control*, John Wiley and Sons, New York, 1959.
[13]Hancock, G. J., "The Static Aeroelastic Deformation of Slender Configurations, Part I: Some Elementary Concepts of Static Deformation," *The Aeronautical Quarterly*, Vol. XII, Aug. 1961, pp. 293–308.
[14]Hancock, G. J., "The Static Aeroelastic Deformation of Slender Configurations, Part II: Some Calculations on Slender Plate Aircraft, Including Non-linear Aerodynamics," *The Aeronautical Quarterly*, Vol. XII, Nov. 1961, pp. 372–394.
[15]Hancock, G. J., "The Static Aeroelastic Deformation of Slender Configurations, Part III: Static Stability," *The Aeronautical Quarterly*, Vol. XIV, Feb. 1963, pp. 75–104.
[16]Hancock, G. J., "The Static Aeroelastic Deformation of Slender Configurations, Part IV: Manoeuvre Theory, "*The Aeronautical Quarterly*, Vol. XIV, Nov. 1963, pp. 311–330.
[17]Diederich, F. W. and Budiansky, B., "Divergence of Swept Wings," TN 1680, Aug. 1948, NACA.
[18]Graham, L. A., Jones, R. T., and Boltz, F. W., "An Experimental Investigation of an Oblique-Wing and Body Combination at Mach Numbers Between 0.60 and 1.40," TM X-62,207, Dec. 1972, NASA

OCTOBER 1973 J. AIRCRAFT VOL. 10, NO. 10

Control System Design Considerations for a Longitudinally Unstable Supersonic Transport

Lloyd R. Tomlinson*
The Boeing Company, Seattle, Wash.

The greatest challenge facing designers of the USA Supersonic Transport was to achieve a design that was economically competitive with the large subsonic transports. In order to achieve this goal, it was necessary to design a Control Configured Vehicle (CCV) which relied on stability augmentation to meet handling qualities and safety requirements. The result was the achievement of significant gains in structural weight and aerodynamic efficiency, netting substantial improvements in range/payload capability. In the process of developing the controls design, several interesting problems were dealt with. New approaches to safety assurance were necessary. The low frequency structural modes imposed constraints on the amount of airframe instability that could be compensated for by the stability augmentation system. Complex augmentation using speed feedback was necessary for complete stability. The augmentation authority and resolution requirements increased significantly. Such problems as nose wheel taxi loads and control forces to rotate for takeoff took on new significance. It is the object of this paper to discuss these problems for possible benefits to future CCV designs.

Introduction

THE effects of transonic flight were particularly apparent for the USA/SST. Figure 1 shows the greatly expanded flight envelope that was planned for the SST. Figures 2 and 3 present typical variations with Mach number of a few key aerodynamic parameters. In the transonic region, large changes occur in all the aerodynamic characteristics, and as Mach number increases to cruise speed, a great reduction takes place in control effectiveness. The large variations in stability, and the reductions in control effectiveness stems from the redistribution of aerodynamic loads in supersonic flow and from aeroelastic distortions. The shift in aerodynamic center with Mach number (Fig. 3) is seen to be of a magnitude three times greater than the allowable loading range for the center of gravity (c.g.).[1]

One of the most critical tasks in the development of an SST configuration is the achievement of satisfactory longitudinal balance. The final arrangement of the airplane must provide an operational c.g. range that satisfies airline requirements for payload loading flexibility while insuring satisfactory longitudinal stability and control and minimum trim drag. Figure 4 illustrates the SST balance problem. Performance, noise, and structural considerations strongly dictated locating the engines on the trailing edge of the wing. This, however, caused a balance problem which would have required a forward extension of the fuselage to provide acceptable c.g. limits for stability if conventional design procedures had been used. The basic problem was that location of the engine masses on the trailing edge of the wing resulted in the Operating Empty Weight (OEW) c.g. being aft of the desired subsonic operating c.g. range. Normal balance could only be

Presented as AIAA Paper 72-871 at the AIAA Guidance and Control Conference, Stanford, Calif., August 14–16, 1972; submitted October 2, 1972; revision received July 16, 1973.
Index categories: Aircraft Configuration Design; Aircraft Handling, Stability and Control; Aircraft Subsystems Design.
*Specialist Engineer, Flight Controls Technology.